Susceptibility loci for murine HIV-associated nephropathy encode trans-regulators of podocyte gene expression

Natalia Papeta,[1] Ka-Tak Chan,[1] Sindhuri Prakash,[1] Jeremiah Martino,[1] Krzysztof Kiryluk,[1]
David Ballard,[2] Leslie A. Bruggeman,[3] Rachelle Frankel,[1] Zongyu Zheng,[1] Paul E. Klotman,[4]
Hongyu Zhao,[2] Vivette D. D'Agati,[5] Richard P. Lifton,[2,6] and Ali G. Gharavi[1]

[1]Department of Medicine, Columbia University College of Physicians and Surgeons, New York, New York, USA. [2]Department of Genetics,
Yale University School of Medicine, New Haven, Connecticut, USA. [3]Department of Medicine, MetroHealth Medical Center,
Case Western Reserve University School of Medicine, Cleveland, Ohio, USA. [4]Department of Medicine, Mount Sinai School of Medicine,
New York, New York, USA. [5]Department of Pathology, Columbia University College of Physicians and Surgeons, New York, New York, USA.
[6]Howard Hughes Medical Institute, Yale University School of Medicine, New Haven, Connecticut, USA.

Multiple studies have linked podocyte gene variants to diverse sporadic nephropathies, including HIV-1–associated nephropathy (HIVAN). We previously used linkage analysis to identify a major HIVAN susceptibility locus in mouse, *HIVAN1*. We performed expression quantitative trait locus (eQTL) analysis of podocyte genes in HIV-1 transgenic mice to gain further insight into genetic susceptibility to HIVAN. In 2 independent crosses, we found that transcript levels of the podocyte gene nephrosis 2 homolog (*Nphs2*), were heritable and controlled by an ancestral cis-eQTL that conferred a 3-fold variation in expression and produced reactive changes in other podocyte genes. In addition, *Nphs2* expression was controlled by 2 trans-eQTLs that localized to the nephropathy susceptibility intervals *HIVAN1* and *HIVAN2*. Transregulation of podocyte genes was observed in the absence of HIV-1 or glomerulosclerosis, indicating that nephropathy susceptibility alleles induce latent perturbations in the podocyte expression network. Presence of the HIV-1 transgene interfered with transregulation, demonstrating effects of gene-environment interactions on disease. These data demonstrate that transcript levels of *Nphs2* and related podocyte-expressed genes are networked and suggest that the genetic lesions introduced by HIVAN susceptibility alleles perturb this regulatory pathway and transcriptional responses to HIV-1, increasing susceptibility to nephropathy.

Introduction

In the past decade, studies in humans and murine models have implicated defects in the glomerular visceral epithelial cells, the podocytes, as a principal factor in the development of nephropathy (1–7). Podocytes are highly differentiated epithelial cells that establish and maintain the glomerular basement membrane and the slit diaphragm. Inherited defects in genes that are specific to or highly expressed in podocytes result in Mendelian forms of nephropathy (e.g., nephrosis 1 homolog [*NPHS1*], *NPHS2*, *ACTN-4*, CD2-associated protein [*CD2AP*], phospholipase C, ε1 [*PLCE1*], *TRPC6*; refs. 1–6). Most recently, 2 studies have also reported strong association of noncoding variants in the podocyte-expressed gene myosin, heavy chain 9, non-muscle (*MYH9*) with susceptibility to primary focal segmental glomerulosclerosis, HIV-1–associated nephropathy (HIVAN), and nondiabetic end-stage renal failure among African Americans (8, 9). These data explain the striking familial aggregation of these pathologically distinct nephropathies among African-Americans (10, 11) and confirm that podocyte defects are a major risk factor for multiple common forms of kidney failure. Interestingly, coding mutations

in *MYH9* cause overlapping dominant syndromic disorders predominantly characterized by macrothrombocytopenia and deafness but can also produce proteinuric nephropathy (May-Hegglin anomaly and Fechtner, Epstein, and Sebastian syndromes; refs. 12–16). The mechanism by which coding or noncoding *MYH9* variants result in diverse nephropathies is not clear.

Several studies have suggested a requirement for gene-gene and gene-environment interaction for determination of complex nephropathy phenotypes (4, 17–20). For example, *Cd2ap* haploinsufficient mice do not develop overt nephropathy but have increased susceptibility to experimental glomerular injury or develop nephropathy in conjunction with a null allele in either the synaptopodin (*Synpo*) gene or the *Fyn* proto-oncogene (4, 21). These data suggest that podocytes can counteract moderate genetic lesions and restore cellular homeostasis without organ failure, but additional insults produce decompensation and disease. From this perspective, genetic susceptibility represents a compensated state that is unmasked upon exposure to additional genetic or environmental insults. However, molecular evidence of a regulated compensatory pathway has not been clearly documented, with genetic interactions being attributed to disruption of physical interaction between encoded gene products (17). Altered expression profiles of podocyte genes have also been demonstrated in humans and animals with genetic or acquired nephropathy (19, 22, 23), but in these settings, primary adaptive changes cannot be differentiated from secondary effects induced by glomerulosclerosis. Identification of such transcriptional networks and their co-regulated com-

Table 1

Significant and suggestive loci for nephropathy-related traits in the TgFVB × B6 F2 intercross

Trait	Chromosome	Location (lod –2), in Mb	lod score	Allele associated with high trait value
Global histology score	13	37–85	4.3[A]	FVB
	4	5–35	2.8 (3.8)[A,B]	B6
Glomerulosclerosis	13	42–82	4.5[A]	FVB
	4	5–35	2.9 (3.7)[A,B]	B6
Tubular dilation/casts	13	37–85	4.3[A]	FVB
	4	5–35	2.3 (3.0)[B]	B6
Tubular degeneration	13	37–80	4.3[A]	FVB
	4	0–44	2.4	B6
Podocyte hypertrophy	13	32–89	3.5[A]	FVB
	7	15–82	2.8	FVB
BUN	13	34–62	2.0	FVB
	3	5–54	1.9	B6
Proteinuria (age 3 wk)	2	74–112	2.3	FVB
	13	54–64	1.8	FVB
Proteinuria (age 12 wk)	12	26–84	3.3	FVB

[A]Statistically significant based on 10,000 permutations of phenotype on genotype. [B]The lod scores in parentheses reflect lod scores on chromosome 4 after adjustment for linkage to chromosome 13.

ponents would provide insight into pathogenic pathways leading to kidney failure in the setting of podocyte mutations.

Combining gene expression profiling with linkage analysis (expression quantitative trait locus [eQTL] mapping) has emerged as a powerful tool for elucidating molecular pathways downstream of disease-causing mutations (24–28). eQTL mapping studies have demonstrated that transcript abundance is an inherited trait that is influenced by local genetic variation in the proximity of the gene locus itself (cis-eQTLs) or by distant loci (trans-eQTLs) that modulate gene expression through chromatin remodeling, transcriptional regulation, or more often, by complex secondary mechanisms (24, 25). Identification of loci that influence both clinical phenotypes and transcript abundance can uncover molecular pathways that link sequence variation to disease (26). For example, given linkage of a gene expression trait and a clinical phenotype to the same locus, statistical models can determine whether the gene expression trait is driving the clinical phenotype or whether variation in the clinical phenotype produces changes in the gene expression trait, resulting in a secondary linkage signal. Thus, the statistical relationship among variation in DNA, gene expression, and clinical phenotypes is utilized to predict directionality among them and infer causal relationships driving the pathogenesis of disease. Because genes that share a common trans-regulator are likely to participate in a functionally related pathway, they can be used to build molecular networks underlying complex traits (26, 29, 30). This approach has been successfully applied to identify genes underlying obesity and metabolic syndrome (29, 30).

Here we apply the eQTL mapping strategy to study mechanisms underlying genetic susceptibility to HIVAN. HIVAN, a major cause of kidney failure in HIV-1 infection, is characterized by collapsing glomerulopathy and microcystic tubular dilatation (31–35). HIV-1 disrupts multiple cellular pathways in podocytes, resulting in enhanced reentry into the cell cycle and loss of expression of signature proteins such as podocin or Synpo, ultimately resulting in proliferation or apoptosis (36–41). A role for host susceptibility factors is demonstrated by increased prevalence among patients of African ancestry, which is strongly attributable to variation in the *MYH9* gene (10, 42, 43) Host predisposition is also reca-

pitulated in murine models of HIVAN, where the development of nephropathy is profoundly influenced by genetic background (38, 44–46). By analysis of genetic linkage in crosses of mouse strains with contrasting susceptibility, we previously localized a major locus for HIVAN, called *HIVAN1*, to chromosome 3A1–A3 (45). Moreover, we found large variation in disease penetrance among inbred strains, implying the existence of additional HIVAN quantitative trait loci (QTLs) that could delineate shared mechanisms underlying susceptibility to HIVAN. Here we show that podocyte gene expression is heritable and that HIVAN susceptibility genes belong to a regulated transcriptional network that modulates expression of podocyte cytoskeletal proteins such as *Myh9* as well as components of the glomerular filtration barrier.

Results

Identification of new HIVAN susceptibility loci in a transgenic FVB/NJ × C57BL/6J F2 intercross. We previously generated a backcross (BC) between HIV-1 transgenic FVB/NJ (TgFVB) and CAST/EiJ (CAST) mice and identified a susceptibility locus for HIVAN on chromosome 3A1–3A3 (called *HIVAN1*) with CAST alleles associated with an increased risk of disease (45). To identify additional nephropathy susceptibility loci, we produced an F2 intercross between TgFVB and the C57BL/6J (B6) strain ($n = 191$) and performed a genome-wide analysis of linkage using 103 informative SNPs to detect loci influencing multiple nephropathy-related phenotypes (histologic injury score, proteinuria, and blood urea nitrogen [BUN]; see Table 1). In this independent cross, there was no evidence of linkage of nephropathy phenotypes to the *HIVAN1* or the *Myh9* loci (on chromosomes 3 and 15, respectively). However, we found significant linkage of histologic injury traits to chromosome 13A3–C2 (the *HIVAN2* locus; peak lod score 4.3 at rs3023383; see Table 1). Linkage to this segment was significant for multiple components of histologic scores and suggestive for BUN and proteinuria. We also identified linkage of histology injury to the centromeric region of chromosome 4A1–A5 (*HIVAN3* locus), where linkage was initially suggestive but achieved genome-wide significance after controlling for the effect of *HIVAN2* (Table 1). The *HIVAN2* and *HIVAN3* loci accounted for 10% and 7%, respectively, of the variance in glomerulosclerosis scores in this cross. Interestingly, at *HIVAN2*, the FVB/NJ (FVB) allele conferred increased risk of renal injury with an additive effect, while at *HIVAN3* the B6 allele conferred increased risk with a recessive effect. We also identified 2 suggestive intervals for proteinuria (chromosomes 2 and 12; Table 1). Together with the initial cross we previously reported (45), these data identify 3 distinct HIVAN susceptibility loci on chromosomes 3A1–A3 (*HIVAN1*), 13A3–C2 (*HIVAN2*), and 4A1–A5 (*HIVAN3*).

HIVAN1 and HIVAN2 influence Nphs2 transcript abundance. To determine whether these HIVAN susceptibility loci were associated with variation in podocyte gene expression, we examined renal expression of *Nphs1*, *Nphs2*, *Cd2ap*, *Actn4*, *Pdxl*, and kin of IRRE like (*Kirrel*) in TgFVB and protected F1 hybrids (F1; FVB × B6, FVB ×
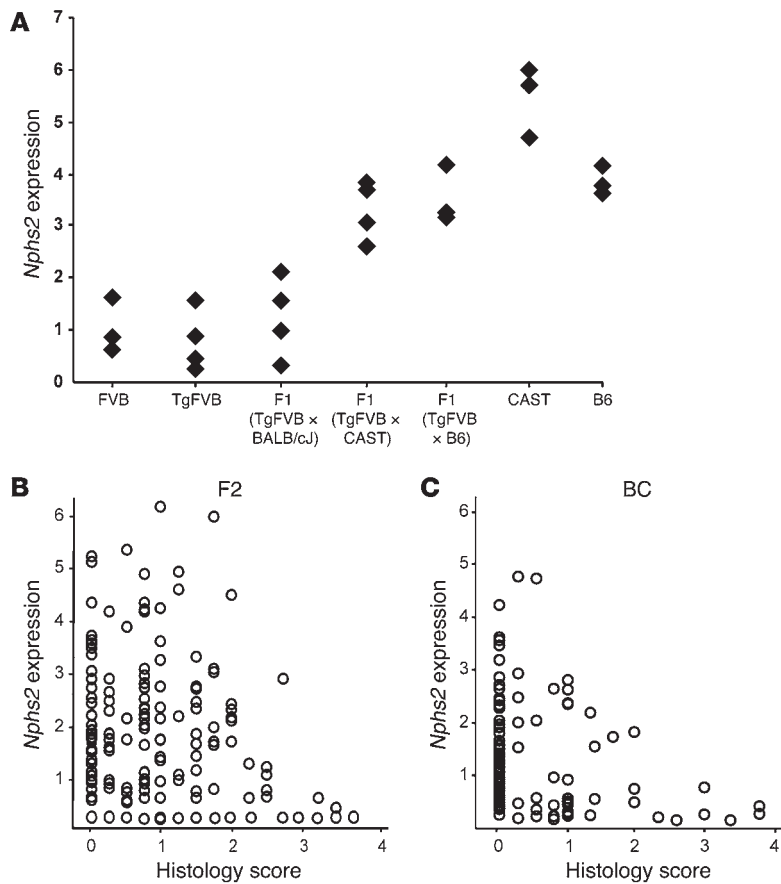
Figure 1
Variation in *Nphs2* transcript abundance and its correlation with renal injury. (**A**) Interstrain variation in *Nphs2* transcript abundance. (**B** and **C**) Distribution of podocin gene expression in HIVAN intercross (F2) and BC in relation to histologic injury score. Each point indicates data from an individual mouse. Expression levels in **A**–**C** are the ratio of expression level of each sample to that of an internal reference sample (FVB).

mosomes 1 and 13 as covariates in the analysis, we identified suggestive evidence for yet another *Nphs2* trans-eQTL on chromosome 3A1–A3 (lod score of 2.4 and 2.1 in F2 and BC, respectively), an interval that corresponds to the *HIVAN1* locus. The cis-eQTL and the trans-eQTLs on chromosomes 13 and 3 account for 40%, 10%, and 4% of the variance in the *Nphs2* transcript level in the F2 cross and 45%, 12%, and 5% of the variance in the BC, respectively. The cis-eQTL and the *HIVAN2* locus achieved genome-wide significance based on published criteria as well as permutation analyses, whereas linkage to the *HIVAN1* locus was suggestive in the 2 independent crosses. Moreover, there was complete overlap in the peak lod scores and the 95th percentile confidence interval for these eQTLs (Figure 2 and Table 1). Therefore, there was remarkable agreement in 2 independent mapping cohorts, demonstrating heritability of *Nphs2* transcript abundance and identifying 2 *Nphs2* trans-eQTLs that coincide precisely with the *HIVAN1* and *HIVAN2* loci.

To determine whether the overlap between eQTLs and nephropathy loci was due to chance, we performed a standard test of linkage versus pleiotropy, in which we tested 2 alternative models: the hypothesis that 2 distinct genes that are closely located within the QTL locus influence each trait separately (linked QTL model) and the null hypothesis that 1 gene in the interval influences both traits (pleiotropic model) (47). Based on this test, the best locations for the QTL position in the 2 models were statistically indistinguishable ($P = 0.6$ and $P = 0.3$ for the *HIVAN1* and *HIVAN2* loci, respectively). As a second statistical approach, simulation studies under the assumption of independence between nephropathy and *Nphs2* traits indicated that the probability of partial or complete overlap of confidence intervals in 2 crosses by chance was 1/200 and 1/5,000, respectively. Therefore, we found no evidence that 2 distinct genes in the HIVAN loci affect HIVAN and *Nphs2* expression separately.

To exclude any confounding effects of kidney injury on findings, we re-examined the *Nphs2* expression data in the subset of mice with normal histology and no proteinuria. The evidence for *Nphs2* cis- and trans-eQTLs remained highly significant, with consistent phenotypic effects across both mapping cohorts ($n = 62$ in BC and $n = 59$ in F2 cross; Figure 3, A–C). This demonstrated that these intervals influence *Nphs2* expression independently of glomerulosclerosis. Moreover, we found that the nephropathy-predisposing alleles were associated with either high (*HIVAN2*) or low (*HIVAN1*) *Nphs2* expression. These data, combined with the absence of linkage of glomerulosclerosis to the strong *Nphs2* cis-eQTL (lod score less than 0.5 in each cross; Figure 2A) indicate that variation in *Nphs2* expression is not a causal factor in the development of glomerulo-

CAST, and FVB × BALB/cJ; refs. 45, 46). Among these genes, only *Nphs2* expression demonstrated significant variation (ANOVA $P < 0.0001$), with levels 3- to 4-fold higher among B6 or CAST F1 hybrids (Figure 1). Measurement in wild-type parental strains demonstrated that this variation was background dependent and unrelated to the presence of the HIV-1 transgene (Figure 1A). We next measured whole-kidney expression of *Nphs2* by quantitative PCR in 145 (TgFVB × B6) F2 intercross mice (F2) and 123 previously produced (TgFVB × CAST) F1 × FVB BC mice (reported in ref. 45). The level of *Nphs2* gene expression was continuously distributed in both cohorts and inversely related to renal injury, suggesting multifactorial determination (quadruplicate measurements; Figure 1, B and C). The variance among mice with no evidence of histologic injury in these crosses was very high compared with the variance in genetically homogeneous strains, or F1s, implying strong genetic regulation of gene expression.

We next performed a genome-wide linkage analysis of *Nphs2* transcript abundance in the F2 and BC mice, with glomerulosclerosis treated as a covariate to adjust for secondary changes in transcript levels due to kidney injury. Remarkably, both cohorts identified the same loci contributing to variation in *Nphs2* gene expression. The first linkage signal localized to within 3 cM of the *Nphs2* gene locus on chromosome 1G3, signifying the presence of a cis-eQTL (lod scores of 20.5 and 7.2 in F2 and BC mice, respectively; Figure 2, A and D). The second peak coincided with the *HIVAN2* locus on chromosome 13A2–C2, identifying a trans-eQTL (lod score of 4.5 and 3.3 in F2 and BC mice, respectively; Figure 2, B and E). In addition, after taking glomerulosclerosis and the eQTLs on chro-

Figure 2
Lod plots for *Nphs2* eQTLs in the F2 and BC cohorts. (**A** and **D**) Linkage of *Nphs2* expression to the *Nphs2* locus on chromosome 1 in F2 and BC. (**B** and **E**) Linkage of *Nphs2* expression to the *HIVAN2* locus on chromosome 13 in F2 and BC. (**C** and **F**) Suggestive linkage of *Nphs2* expression to the *HIVAN1* locus on chromosome 3 in F2 and BC (after adjustment for the chromosomes 1 and 13 eQTLs). The positions of informative markers are shown above each plot. The dashed horizontal lines indicate the thresholds for genome-wide significance (3.6 in F2 and 2.9 in BC). The bars above the lod plot indicate the 95th percentile confidence interval for each trait locus. The location of *Nphs2* is shown above the lod plot for chromosome 1. The 95th percentile confidence intervals for the *Nphs2* eQTLs were: on chromosome 1, 142–162 (F2) and 140–174 Mb (BC); on chromosome 13, 36–79 Mb (F2) and 32–84 Mb (BC); on chromosome 3, 6–48 Mb (F2) and 6–64 Mb (BC).

sclerosis. The alternative explanation is that the linkages of *Nphs2* expression to HIVAN loci represent reactive or regulatory responses to perturbations produced by HIVAN susceptibility alleles. The presence of such a regulatory response can be prospectively tested by determining whether introduction of a known genetic perturbation (i.e., the *Nphs2* cis-eQTL) results in altered expression of additional podocyte genes and whether this response is similar to genetic profile elicited by HIVAN susceptibility alleles.

Tightly linked sequence variants at the Nphs2 locus are associated with a 3-fold difference in transcript level, producing perturbations in other podocyte genes. We initially investigated the *Nphs2* cis-eQTL because it contributes a 3- to 4-fold difference in transcript level and can validate the hypothesis of a reactive response in podocyte genes. To verify that *Nphs2* expression is affected by one or more cis- variants, we sequenced the *Nphs2* gene (2.5-kb sequence upstream of the

start codon, the exons, and 3′ UTR) in 19 inbred strains, including the 3 parental strains with contrasting expression profile. We identified a larger than expected number of sequence variants among the strains tested, including a total of 103 SNPs and 13 insertions/deletions. Among these were 4 non-synonymous SNPs and 2 exonic insertions/deletions (s 2–4). The SNP density in the *Nphs2* locus was 1 variant per approximately 36 bp surveyed, which is 8-fold higher than the genome-wide average for inbred strains (48). Phylogenetic analysis demonstrated that these SNPs were not randomly distributed but clustered into 3 major haplotypes that corresponded to the ancestral genomes of the laboratory mouse (*Mus musculus domesticus*, *Mus musculus musculus*, and *Mus musculus castaneus*; Figure 4A). The *M.m. musculus* haplotype differed from the *M.m. domesticus* and *M.m. castaneus* strains by 60 and 77 sequence variants, respectively, while the latter 2 were dis-
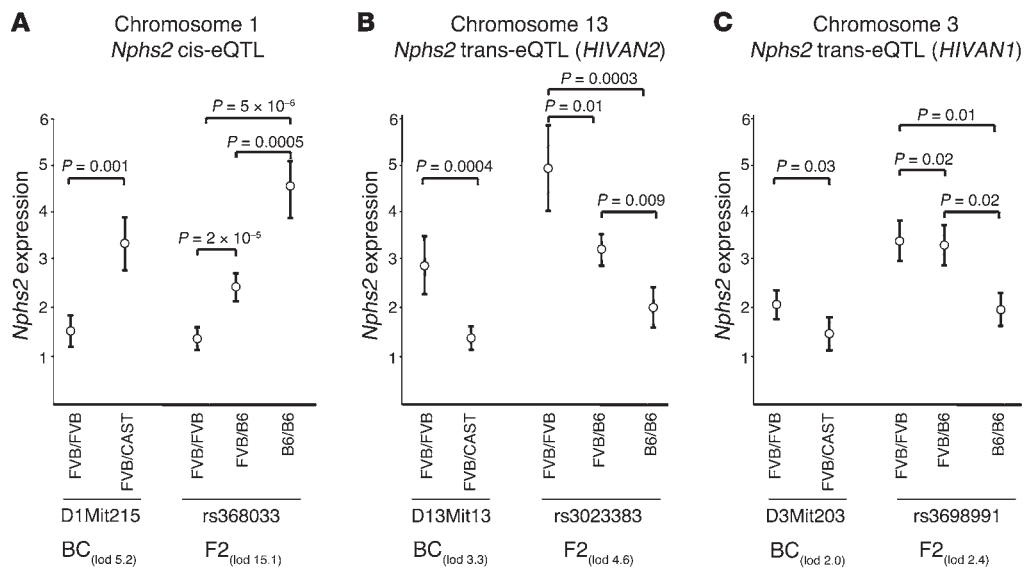
Figure 3
Nphs2 expression levels at each eQTL in BC (*n* = 62) and F2 (*n* = 59) mice with no evidence of renal disease. (**A**) Cis-eQTL on chromosome 1. (**B** and **C**) Trans-eQTL on chromosomes 13 (**B**) and 3 (**C**). The expression value for the *HIVAN1* locus on chromosome 3 was adjusted for chromosome 1 and chromosome 13 eQTLs. Expression levels in **A**–**C** are the ratio of the expression level of each sample to that of an internal reference sample (FVB). The genotypes and markers at the locus are indicated on the *x* axis. Data are mean ± SEM.

tinguished by 31 sequence variants. In addition, we observed a substantial number of private intrasubspecific variants. Notably, we found a 30-bp in-frame deletion in exon 1 in the B6, SJL/J, and CFW strains that was absent in other inbred strains, including the wild-derived strains representative of the ancestral mouse genomes (PWD/PhJ, CAST, and WSB/EiJ), indicating that the deletion occurred during the derivation of inbred strains. The combination of high SNP density and the occurrence of new intrasubspecific SNPs indicate that the *Nphs2* sequence has experienced an unusually high mutation rate across the mouse lineage. We calculated the ratio of non-synonymous (Ka) to synonymous (Ks) nucleotide substitution rates to determine whether the high polymorphism rate can be explained by positive selection of *Nphs2*. However, the Ka/Ks ratio across all amino acid sites in *Nphs2* was 0.33 (Ka/Ks >1 is indicative of positive selection) and a whole gene likelihood ratio test showed no evidence to support positive selection (*P* = 0.30).

We next performed an association study of the 3 *Nphs2* haplotypes with transcript abundance (Figure 4B). The *Nphs2* haplotypes explained 40% of the variance among inbred strains. The strains with the *M.m. musculus* haplotype (FVB/NJ [FVB], C3H/HeJ, CBA/J, A/J, DBA/2J, RIIIS/J, and BALB/cJ) demonstrated 3-fold lower expression of *Nphs2* compared with the strains with the *M.m. domesticus* haplotype (B6, C57BL/10J, SJL/J, CFW, and 129/SvEv; *P* = 3 × 10^{-12}), while there were no significant differences between strains carrying the *M.m. domesticus* and *M.m. castaneus* haplotypes (*P* = 0.1). Western blot analysis in the representative strains confirmed gene expression data classifying the same strains into high- and low-expression groups (Figure 4C). We also conducted 5′ and 3′ RACE in B6 and FVB strains but found no evidence of alternative transcripts. These data provide clear evidence that the large variance in *Nphs2* expression among inbred strains is attributable to one or more sequence variants within this locus.

To study the trans-regulatory effects of the *Nphs2* cis-eQTL and test the hypothesis of a networked response in podocyte genes, we examined B6-chr01^A–consomic strains, in which chromosome 1 from the A/J strain (low-expression haplotype) was substituted into the B6 (high-expression haplotype) genome (Figure 5A). As predicted by the linkage and inbred strain data, substitution of chromosome 1 from A/J into the B6 genome resulted in a primary reduction in *Nphs2* expression (3-fold difference for the B6-chr01^A strain compared with the B6 reference strain; *P* = 10^{-7}) but no overt evidence of nephropathy. We next examined whether this primary decrease in *Nphs2* is associated with altered expression of its known interacting partners (*Nphs1*, *Cd2ap*, and *Kirrel*) as well as other podocyte-expressed genes (*Plce1*, *Myh9*, Wilms tumor 1 homolog [*Wt1*], and *Synpo*). Compared with the B6 reference strain, B6-chr01^A exhibited 1.3- to 2.8-fold increased expression of *Myh9* (*P* = 5 × 10^{-7}), *Synpo* (*P* = 0.006), *Nphs1* (*P* = 0.04), *Plce1* (*P* = 0.004), and *Kirrel* (*P* = 0.005) but no changes in *Cd2ap* or *Wt1* transcript (Figure 5A). Importantly, although we tested only 3 intervals and 1 consomic substitution, the *Myh9* and *Plce1* comparisons reached genome-wide significance levels for mapping in 20 consomic strains (*P* < 0.004) (49). Thus, in response to a primary genetic perturbation in *Nphs2*, we observed a significant augmentation in expression of multiple podocyte genes involved in the composition and regulation of the slit diaphragm. Because the altered transcripts are not encoded on chromosome 1, variation in their expression can only be attributed to trans-regulation. Moreover, since the B6-chr01^A mice did not have nephropathy, these findings are independent of the confounding effects of glomerulosclerosis and establish normative data about podocyte response to a primary decrease in *Nphs2* expression.

HIVAN1 and HIVAN2 susceptibility alleles activate the same podocyte regulatory pathway as the hypomorphic Nphs2 allele. We next determined whether HIVAN susceptibility genes also activate the same regulated pathway by studying 2 inbred strains harboring genomic

A
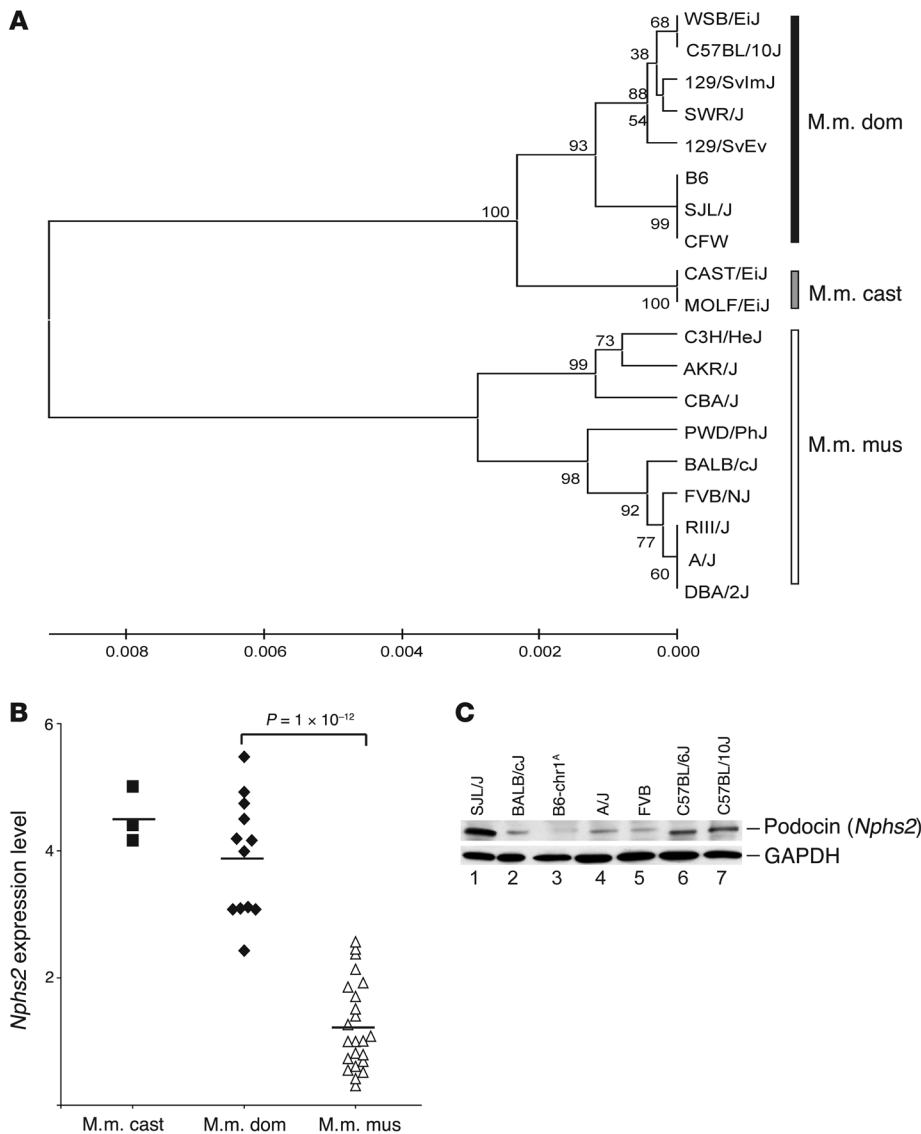
Figure 4
Podocin (*Nphs2*) level is associated with mouse ancestral haplotype. (**A**) Phylogeny of the *Nphs2* sequence identified 3 major clades among 19 inbred strains. Numbers indicate the percentages of replicate trees in which the associated taxa clustered together in the bootstrap test (10,000 replicates). Scale indicates branch lengths and the evolutionary distances, measured as the number of base substitutions per site. (**B**) *Nphs2* expression level in inbred mice was significantly associated with haplotype. Individual points indicate *Nphs2* levels in mice of various strains, grouped by ancestral haplotype, with means shown for each group. Expression levels are shown as the ratio of the expression level of each sample relative to that of an internal reference sample (FVB). (**C**) Western blot analysis of podocin levels in the kidney of representative mouse strains confirmed quantitative PCR data. Positions of podocin and GAPDH (loading control) are indicated. M.m. mus, *M.m. musculus*; M.m. cast, *M.m. castaneus*; M.m. dom, *M.m. domesticus*.

B

C

substitution encompassing the *Nphs2* trans-eQTLs (*HIVAN1* and *HIVAN2* loci). To examine the trans-regulatory effects exerted by the *HIVAN2* locus, we studied B6-chr13[A] mice, in which chromosome 13 from the A/J genome was substituted into the B6 genome. These consomic strains were suitable because A/J and FVB strains both have the low-expression haplotypes at the cis-eQTL, and *Nphs2* expression levels are nearly identical between them (Figure 4), suggesting that they also share the same alleles at the *Nphs2* trans-eQTL. As predicted, B6-chr13[A] mice demonstrated a 2-fold increase in *Nphs2* transcript abundance ($P = 2 \times 10^{-8}$ versus the B6 strain; Figure 5B). In addition, this genomic substitution was characterized by 1.3- to 2.7-fold increased expression of *Myh9* ($P = 0.008$), *Nphs1* ($P = 5 \times 10^{-6}$), *Cd2ap* ($P = 0.0008$), *Kirrel* ($P = 0.017$), *Plce1* ($P = 0.008$), and *Synpo* ($P = 0.03$) but no changes in *Wt1* expression. The *Myh9* and *Nphs1* comparisons reached genome-wide significance levels for mapping in 20 consomic strains (49). These data confirmed our initial hypothesis that HIVAN susceptibility alleles modify podocyte gene expression independent of HIV-1 and the *Nphs2* cis-eQTL. Moreover, this augmented expression

closely resembles the profile observed in B6-chr01[A] mice, which have a primary decrease in *Nphs2* expression. This similarity in gene expression response suggests that the *HIVAN2* susceptibility alleles produce a genetic lesion that resembles a reduction of *Nphs2* expression and that the *Hivan2*, *Myh9*, and *Nphs2* genes belong to a common regulatory pathway.

We next examined the expression profile elicited by *HIVAN1* susceptibility alleles. We generated *HIVAN1* congenic mice by introgressing approximately 52 Mb of the CAST genome at the *HIVAN1* locus into the FVB genetic background (FVB-*HIVAN1*[CAST] mice). HIV-1 transgenic FVB-*HIVAN1*[CAST] mice develop accelerated renal failure compared with TgFVB, but their nontransgenic counterparts are viable and phenotypically normal (50). However, examination of renal gene expression in nontransgenic congenic mice demonstrated that CAST alleles at the *HIVAN1* locus result in a significant reduction in baseline expression of *Nphs2* ($P = 0.04$) and *Kirrel* ($P = 0.001$) compared with the FVB strain (Figure 5C). Moreover, CAST alleles were also associated with significantly increased expression of *Myh9* ($P = 0.01$) but no changes in *Cd2ap*,
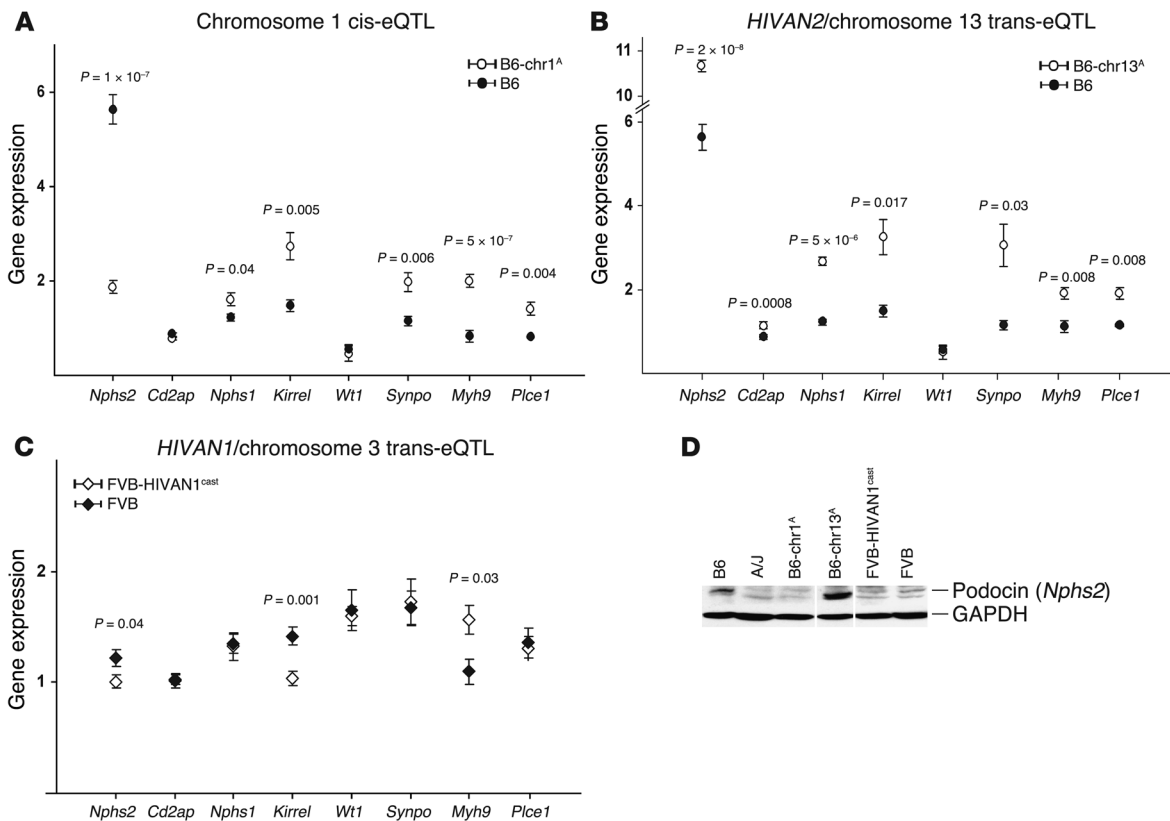
Figure 5
Distinct expression profile of podocyte genes in the congenic and consomic strains harboring *Nphs2* eQTLs compared with their respective reference strains. (**A**) *Nphs2* cis-eQTL. (**B**) HIVAN2/chromosome 13 trans-eQTL. (**C**) HIVAN1/chromosome 3 trans-eQTL. Data are mean ± SEM. Expression levels in **A**–**C** are shown as the ratio of the expression level of each sample to that of an internal reference sample (FVB). (**D**) Western blot analysis demonstrated concordance of quantitative PCR and protein expression levels for podocin. *P* values for comparison with reference strains are shown for each transcript. B6 (*n* = 10), FVB (*n* = 20), B6-chr1^A (*n* = 6), B6-chr13^A (*n* = 4), and FVB-HIVAN1^{CAST} (*n* = 20).

Nphs1, *Plce1*, *Synpo*, or *Wt1* transcript levels. This gene expression profile is qualitatively different from the response observed at the *Nphs2* cis-eQTL or the *HIVAN2* locus, suggesting that the *HIVAN1* susceptibility allele produces a different defect in podocytes.

Altogether, after interrogating 3 genomic segments (corresponding to 372 Mb or ~12.3% of the mouse genome), we identified 16/24 transcripts with significant differences in expression at $P < 0.04$, whereas 1 significant difference would have been expected by chance (false discovery rate = 0.06). Moreover, each interval tested was significant for at least 3 expression traits and, conversely, 6/8 interrogated transcripts were significant in at least 2 intervals. Finally, 7/24 comparisons (including 2 for *Nphs2*) reached genome-wide significance for mapping in consomic strains ($P < 0.004$; ref. 49). The possibility of multiple independent eQTLs that influence each podocyte transcript separately cannot be formally excluded without fine mapping of each congenic/consomic interval. However, based on the genome-wide density and frequency of trans-eQTLs reported in one of the largest studies in the mouse (28), we estimate that the probability of chance detection of 5 genome-wide significant trans-eQTLs that are independent of *Nphs2* trans-eQTLs is 3×10^{-5}. Thus, the most parsimonious explanation for our findings is that the same eQTL within each region jointly influences expression of *Nphs2* and other podocyte genes.

To complete these studies, we determined whether the podocyte expression profile is modified in the presence of HIV-1 by examining HIV-1 transgenic FVB-HIVAN1^{CAST} and TgFVB mice. To minimize secondary effects of glomerulosclerosis on gene expression, ten 6-week-old transgenic mice of each genotype were matched for age, gender, and degree of renal injury (range of 9%–55% glomerulosclerosis). HIV-1 resulted in reduced expression of *Myh9*, *Nphs1*, and *Wt1* in both genotype groups. On the other hand, we found a reciprocal change in the *Cd2ap*, *Synpo*, *Plce1*, and *Kirrel* response according to *HIVAN1* genotype (Figure 6). Compared with their nontransgenic counterparts, HIV-1 transgenic mice with the FVB alleles (protective) exhibited significantly increased expression of *Kirrel* ($P = 0.01$) and *Cd2ap* ($P = 0.001$) and no change in *Synpo* or *Plce1*. In contrast, mice harboring the nephropathy-prone CAST alleles demonstrated no change in *Kirrel* or *Cd2ap* transcript levels and a significant decrease in *Synpo* ($P = 0.004$) and *Plce1* ($P = 0.01$) expression. These data remained significant after adjustment for degree of glomerulosclerosis and HIV-1 transgenic status, suggesting that interaction of HIV-1 with *HIVAN1* alleles selectively blunts upregulation of *Kirrel* and *Cd2ap* while promoting downregulation of *Synpo* and *Plce1*. These data demonstrate that the podocyte gene expression is strongly modified by the presence of HIV-1 and by underlying *HIVAN1* genotype.
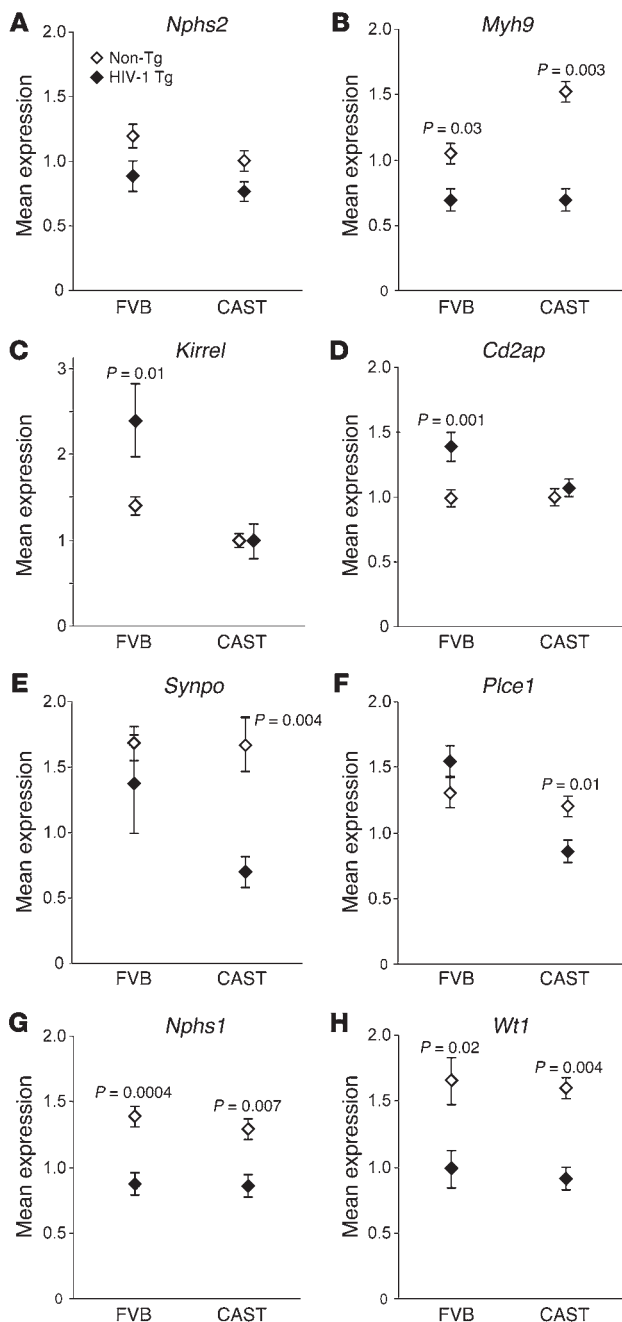
Figure 6
Expression of podocyte genes is altered by the *HIVAN1* genotype and further modified in the presence of the HIV-1 transgene. The *HIVAN1* genotype is shown on the *x* axis (FVB, protective allele; CAST, susceptible allele). The expression levels (mean ± SEM) of each podocyte transcript in wild-type (non-Tg, open symbols) and HIV-1 transgenic (filled symbols) are shown. Significant *P* values for comparison between transgenic and nontransgenic mice within the same genotype group are indicated. While *Nphs2* (**A**), *Myh9* (**B**), *Nphs1* (**G**), and *Wt1* (**H**) showed downregulation in the presence of HIV regardless of genotype, there was a differential response to the HIV-1 transgene according to *HIVAN1* genotype for *Kirrel* (**C**), *Cd2ap* (**D**), *Synpo* (**E**), and *Plce1* (**F**) expression. Expression levels are shown as the ratio of the expression level of each sample to that of an internal reference sample (FVB). FVB ($n = 20$), TgFVB ($n = 10$), FVB-HIVAN1^{CAST} ($n = 20$), and TgFVB-HIVAN1^{CAST} ($n = 10$).

pattern of the linkage data did not support a causal relationship between variation in *Nphs2* expression and glomerulosclerosis, we inferred that the transregulation of *Nphs2* must represent reactive or compensatory changes secondary to genetic lesions introduced by the HIVAN susceptibility alleles. This suggested that expression of podocyte genes is networked and responsive to genetic perturbations. We validated this hypothesis by examining the transcriptional response to the naturally occurring *Nphs2* hypomorphic allele, demonstrating significant upregulation of multiple podocyte genes whose products have direct and indirect physical association with *Nphs2* (*Nphs1*, *Kirrel*, *Myh9*, *Plce1*, and *Synpo*). Furthermore, nontransgenic *HIVAN1* congenic and chromosome 13–consomic mice demonstrated upregulation of the same podocyte transcripts, placing murine HIVAN susceptibility genes within the same regulatory network that includes *Nphs2*, *Myh9*, and related components of the glomerular filtration. The identification of distinct but related molecular phenotypes for *HIVAN1* and *HIVAN2* further suggested that the underlying susceptibility genes introduce different lesions within this common regulatory pathway.

These data can be interpreted without the confounding effects of glomerulosclerosis or HIV-1 gene products, demonstrating that podocytes can modulate the expression of key components of the glomerular filtration barrier in response to genetic lesions. This concept can explain the seemingly contradictory finding that HIVAN susceptibility alleles were associated with both low (*HIVAN1*) and high (*HIVAN2*) *Nphs2* expression. These differing expression profiles likely represent different modes of a regulatory pathway that is responding to distinct genetic perturbations introduced by *HIVAN1* and *HIVAN2* susceptibility alleles. Additional studies can determine whether this altered podocyte gene expression profile is merely reactive or indicative of a compensatory response that enables restoration of podocyte homeostasis. It is also important that upon introduction of HIV-1, *HIVAN1* susceptibility alleles produced a very different gene expression profile compared with protective alleles, suggesting that gene-environment (e.g., viral genome) interactions disturb the regulatory network and produce the dysregulated podocyte phenotype that contributes to the development of nephropathy. One can postulate that similar events occur in the presence of *MYH9* susceptibility alleles in humans, initiating the development of nephropathy. This hypothesis can be tested by examination of *Myh9* haploinsufficient mice, which are phenotypically normal (51, 52), to determine whether they display a renal molecular signature similar to the

Discussion

In the present study, we demonstrate that genetic susceptibility to HIVAN is a latent state characterized by downstream perturbations in podocyte expression profile. We started with identification of 2 QTLs for HIVAN and demonstrated strong heritability of *Nphs2* transcript abundance across inbred strains with different susceptibility to HIVAN. Studies in 2 independent mapping cohorts demonstrated that variation in *Nphs2* expression is controlled a cis-eQTL and 2 trans-eQTLs. While the *Nphs2* cis-eQTL did not influence the development of glomerulosclerosis, the trans-eQTLs both coincided with susceptibility loci for HIVAN (*HIVAN1* and *HIVAN2*), suggesting identity between genes influencing *Nphs2* transcript abundance and nephropathy. Because the

congenic/consomic mice studied here and whether they develop nephropathy with appropriate environmental insults. Moreover, Ratelade et al. have recently identified modifier loci influencing proteinuria and kidney function in *Nphs2*-null mice and further demonstrated that maternal-fetal factors also profoundly modify these phenotypes (53). The nephropathy QTLs in the *Nphs2*-null mice are distinct from the HIVAN susceptibility loci but also include some podocyte-expressed genes (*Synpo2* on chromosome 3 and *Iqgap1* on chromosome 7). Thus, it would be interesting to know whether the modifier loci identified in *Nphs2*-null mice control the expression of other podocyte genes.

Our eQTL study provides a framework for systematic reconstruction of the molecular network connecting to HIVAN susceptibility alleles, *Myh9*, and other nephropathy-associated genes. For example, comprehensive renal expression profiling can uncover differentially expressed genes that the congenic/consomic mice have in common, identifying critical components of this regulatory pathway, while mapping studies can determine whether additional trans-eQTLs (in the substituted segments or elsewhere in the genome) influence the expression of podocyte transcripts, dissecting intermediate nodes in the network. In addition, genome-wide expression profiling in the F2 and BC mapping cohorts can identify the full network of genes that are transregulated by HIVAN loci, detecting causal mediators of disease and HIV-1–induced perturbations in these pathways. This approach can also identify cis-eQTLs that localize to the *HIVAN1* and *HIVAN2* intervals, thereby isolating strong positional candidates for nephropathy. Similar analytic approaches have recently been applied to dissect other complex traits, such as a chromosome 1 QTL associated with multiple metabolic- and obesity-related traits, where expression traits linking to this interval were decomposed into causal or reactive phenotypes, leading to identification of multiple interconnected genes that mediate disease (29, 30).

Although the *HIVAN1* and *HIVAN2* loci contain several transcription factors, none have a predicted binding site on the *Nphs2* promoter. Conversely, none of the transcription factors that are known to regulate *Nphs2* map to HIVAN loci (*Foxc2* is on chromosome 8 [ref. 54] and *Lmx1b* is on chromosome 2 [ref. 55]). These data are consistent with published eQTL studies that have indicated that trans-eQTL intervals encode many different gene classes, such as transcription factors, microRNAs, ligands, receptors, enzymes, substrates, or subunits of protein complexes that can affect their target transcript via a context-dependent mechanism (26, 56, 57). These studies have also shown that functional variants underlying cis-eQTLs often involve multiple linked polymorphisms resulting in haplotype effects (58–60). This situation is illustrated by the analysis of the *Nphs2* cis-eQTL, in which the large number of sequence variants differentiating haplotypes with a contrasting expression profile suggested the potential for multiple functional alleles. It is also noteworthy that the 26-Mb region encompassing the *Nphs2* locus is enriched for genes related to immunity, defense, and olfaction, which are subject to strong positive selection and rapid evolution among most species. We found no evidence for positive selection of *Nphs2* based on absence of excess non-synonymous substitutions. Additional sequence analysis of neighboring genes will be required to determine whether positive selection operated on other genes in this region, providing a permissive setting for accumulation of sequence variants in *Nphs2* (61). These complexities of the mouse *Nphs2* locus present several opportunities for studying gene regulation. Because identified variants are associated with substan-

tial in vivo differences in transcript and protein abundance, they offer an attractive catalog of functional candidates whose individual roles can be dissected by traditional promoter analysis. In particular, among the 116 *Nphs2* sequence variants we describe, 3 missense variants and a 21-bp deletion upstream of the transcription start site in the low-expression haplotype are promising functional candidates (s 2–4). Conversely, promoter segments devoid of SNPs may point to evolutionary conserved regulatory modules that direct podocyte-specific expression.

Our eQTL study presents a survey of the podocyte transcriptional response to nephropathy predisposing alleles, demonstrating the importance of underlying genotype and environment in interpreting the relationship of the gene expression profile to nephropathy. These studies outline a framework for reconstruction of the molecular networks connecting diverse glomerulopathy-associated genes. Identification of podocyte transregulators and their associated network will provide insight into the pathogenesis of multiple forms of primary and secondary nephropathy.

Methods

Animal breeding. All inbred strains (including consomic lines) were purchased from The Jackson Laboratory. The HIV-1 transgenic mouse line TgN(pNL43d14)26Lom 26 (TgFVB) was produced on the inbred FVB/N genetic background and has been extensively characterized (44, 45). The TgFVB × (FVB × CAST) F1 BC has been previously reported (45). A second mapping cohort was produced for this study by intercrossing TgFVB × B6 F1 hybrids (F2 cohort) and phenotyped at 12 weeks of age. Animals that were moribund were euthanized prior to this end point. As before (45), 3 primary phenotypes related to renal disease were characterized: renal histology, BUN, and proteinuria. Proteinuria was measured by spot urine dipsticks (Roche) at 3 and 12 weeks of age. Congenic mice for the *HIVAN1* locus were generated by 10 generations of backcrossing to FVB. The proximal and distal ends of the congenic intervals were delimited by markers D3Mit61 (5.1 Mb) and D3Mit69 (57 Mb), respectively. Successful introgression of this interval into the FVB genetic background was further confirmed by typing 82 informative loci across the genome in the tenth generation. For gene expression studies, mice were studied at 6–8 weeks of age. We profiled whole kidney in 40 nontransgenic mice and 20 HIV-1 transgenic mice equally distributed across *HIVAN1* genotype and gender. To minimize secondary effects of glomerulosclerosis on gene expression, the HIV-1 transgenic mice of each *HIVAN1* genotype were matched for age and degree of renal injury (range 9%–55% glomerulosclerosis). To study the *HIVAN2* locus and the *Nphs2* cis-eQTL, we compared 4 B6-chr13[A] (all female) and 6 B6-chr01[A] mice (3 male /3 female) to 10 wild-type B6 mice (5 male /5 female). Renal histology was scored independently by an investigator blinded to genetic background and other traits. Three traits related to tubulointerstitial disease (epithelial regeneration/degeneration, tubular casts and dilatation, and interstitial infiltrates) and 3 related to glomerular injury (glomerular sclerosis and podocyte hyperplasia and collapse) were scored using a semi-quantitative scale: 0, no disease; 1, 1%–25% of tissue showing abnormalities; 2, 26%–50% of tissue showing abnormalities; 3, 51%–75% of tissue showing abnormalities; and 4, >75% of tissue showing abnormalities. A global histologic score was calculated as an average of 6 renal injury scores. The protocol was approved by the IACUC at the Columbia University Medical Center.

Measurement of podocyte gene expression. We examined *Nphs2* expression in whole kidney because the gene is exclusively expressed in the glomerulus and demonstrated strong heritability from whole kidney measurements of inbred strains. Moreover, the acquisition of whole kidney tissue greatly minimizes the chance of producing secondary changes in gene expression

compared with glomerular isolation procedures. Total RNA was extracted from mouse kidneys using TRIzol reagent (Invitrogen), followed by treatment with DNaseI and clean-up using the RNeasy kit (QIAGEN) according to the manufacturers' protocols. cDNA was generated with the Omni-Script kit (Qiagen). Gene expression was quantitated in quadruplicate by quantitative PCR using SYBR Green mix on an IQ thermal cycler (Bio-Rad). Values were standardized to an internal control, a reference sample (a male FVB) included in each run, and β-actin was used as housekeeping control (using the Pfaffl algorithm; ref. 62). Primer sequences and PCR conditions are included in Supplemental Table 1 (supplemental material available online with this article; doi:10.1172/JCI37131).

Genotyping and analysis of linkage. The BC group had been previously genotyped using microsatellites across the mouse autosomes (45). The F2 cohort was genotyped using 103 informative SNPs across mouse autosomes (Kbiosciences). Pairwise and multipoint likelihood ratio statistics (LRSs) and the proportion of the variance of each trait explained by each trait locus were calculated using the QTX 20 program under an additive model (BC) and a free model (F2 cross) (63). Traits were adjusted for significant covariates by analysis of residuals. Lod scores were calculated by dividing the LRS by 4.6, and traditional thresholds for significance in the BC and intercross were used (lod score >3.3 and >4.3, respectively) (64). In addition, we conducted 10,000 permutations of phenotypes on genotype to determine the empirical significance of the linkage findings. Significant linkage threshold was defined as the lod value that would be expected to occur by chance in 1 of 20 genome scans. Suggestive linkage was defined as the lod value that would be expected to occur at random once per genome scan. Confidence intervals were derived by bootstrap tests. The results of the analysis were also confirmed using the R/QTL package (http://www.rqtl.org/download/; ref. 65) and the Haley-Knott regression method. We performed a standard test of linkage versus pleiotropy to determine whether the coincident linkage peaks for HIVAN and the *Nphs2* transcript level were due to chance or attributable to pleiotropic effects of the same gene affecting both traits (47). In this analysis, we tested the hypothesis that 2 distinct genes that were closely located within the QTL locus influence each trait separately (linked QTL model) against the hypothesis that 1 gene in the interval influences both traits (pleiotropic QTL model). An LRS was computed for the linkage versus pleiotropy models, testing whether the best locations for the 2 QTL models were the same. A parametric bootstrap procedure was performed to obtain the null distribution. *P* values less than 0.05 provided statistically significant evidence against the pleiotropic model. As a second approach for examining the possibility of chance overlap, we assumed complete independence between the nephropathy and *Nphs2* expression traits and performed simulation studies in an F2 and a BC cohort of the same size as in our study. We first fixed the location of the HIVAN loci in each cross. We next performed 10,000 simulated genome scans containing 2 QTLs with the same effect size and confidence intervals as the *Nphs2* trans-eQTLs and randomly permutated the location of these eQTLs across the genome to determine how frequently confidence intervals demonstrate partial overlap (defined as >10 cM overlap) or complete overlap (best position within 5 cM of each other). To test whether the data in congenic or consomic strains could be explained by multiple independent eQTLs within the substituted segments, we used the largest published

mouse genome study (28) to estimate the density of trans-eQTLs across the genome and the a priori probabilities that a given transcript had a trans-regulator. The probability of detection of 5 independent genome-wide significant trans-eQTLs for 21 independent comparisons within the tested segment was derived from the binomial distribution.

Sequencing and 5′ RACE and 3′ RACE. The *Nphs2* gene was sequenced in 19 inbred strains (2.5 kb upstream sequence upstream of the start codon, exons, and 3′ UTR), and sequence traces were aligned and analyzed using the Sequencher 4.7 program (Gene Codes Corp.). Polymorphism data are reported in Supplemental Tables 2–4 and also submitted to GenBank (accession numbers: FJ715751–FJ715776 and FJ717826–FJ717833). 5′ RACE and 3′ RACE experiments were performed according to the manufacturer's protocols (Ambion). TOPO TA cloning of the resulting PCR fragments into the pCRII vector (Invitrogen) with followed by sequencing confirmed identified variants.

Western blotting. Whole kidney lysates (100 μg of total protein per well) were separated in 7.5% SDS-PAGE and transferred onto nitrocellulose membrane. Detection of proteins of interest was performed using Immobilon Western ECL detection kit (Millipore) and the following antibodies: polyclonal rabbit anti-podocin (Sigma-Aldrich), mouse monoclonal anti-GAPDH (R&D Systems), and HRP-labeled sheep anti-mouse (Amersham Biosciences) or goat anti-rabbit (Jackson ImmunoResearch Laboratories Inc.) antibody.

Statistical and bioinformatics analysis. Statistical analyses were performed using SPSS version 15.0. Quantitative traits in the F2 group were compared using *t* tests and ANOVA. Gene expression values among inbred strains were compared using a 2-sided *t* test. The generalized linear model procedure was used for analysis of gene expression in HIV-1 transgenic *HIVAN1* congenic mice, adjusting for glomerulosclerosis. *P* values ≤ 0.05 were considered significant. Phylogenetic analyses of *Nphs2* sequences were performed using the MEGA 4.0 program (http://www.megasoftware.net/; ref. 66), using the unweighted pair group method with arithmetic mean (UPGMA) algorithm. In order to evaluate whether the high mutation rate in the *Nphs2* gene was due to positive selection, we estimated the ratio of non-synonymous (Ka) to synonymous (Ks) nucleotide substitution rates for each amino acid site within the *Nphs2* gene based on the analysis of homologous coding sequences from 10 different strains (67).

Address correspondence to: Ali G. Gharavi, Department of Medicine, Columbia University College of Physicians and Surgeons, 1150 St. Nicholas Ave., Russ Berrie Pavilion 302, New York, New York 10032, USA. Phone: (212) 851-5556; Fax: (212) 305-5520; E-mail: ag2239@columbia.edu.

1. Kestila, M., et al. 1998. Positionally cloned gene for a novel glomerular protein — nephrin — is mutated in congenital nephrotic syndrome. *Mol. Cell.* **1**:575–582.
2. Kaplan, J.M., et al. 2000. Mutations in ACTN4, encoding alpha-actinin-4, cause familial focal segmental glomerulosclerosis. *Nat. Genet.* **24**:251–256.
3. Boute, N., et al. 2000. NPHS2, encoding the glomerular protein podocin, is mutated in autosomal recessive steroid-resistant nephrotic syndrome. *Nat. Genet.* **24**:349–354.
4. Kim, J.M., et al. 2003. CD2-associated protein haploinsufficiency is linked to glomerular disease susceptibility. *Science.* **300**:1298–1300.
5. Winn, M.P., et al. 2005. A mutation in the TRPC6 cation channel causes familial focal segmental glomerulosclerosis. *Science.* **308**:1801–1804.
6. Hinkes, B., et al. 2006. Positional cloning uncovers mutations in PLCE1 responsible for a nephrotic syndrome variant that may be reversible. *Nat. Genet.* **38**:1397–1405.
7. D'Agati, V.D. 2008. Podocyte injury in focal segmental glomerulosclerosis: Lessons from animal models (a play in five acts). *Kidney Int.* **73**:399–406.
8. Kao, W.H., et al. 2008. MYH9 is associated with nondiabetic end-stage renal disease in African Americans. *Nat. Genet.* **40**:1185–1192.

9. Kopp, J.B., et al. 2008. MYH9 is a major-effect risk gene for focal segmental glomerulosclerosis. *Nat. Genet.* **40**:1175–1184.

10. Freedman, B.I., Soucie, J.M., Stone, S.M., and Pegram, S. 1999. Familial clustering of end-stage renal disease in blacks with HIV-associated nephropathy. *Am. J. Kidney Dis.* **34**:254–258.

11. Freedman, B.I., Soucie, J.M., and McClellan, W.M. 1997. Family history of end-stage renal disease among incident dialysis patients. *J. Am. Soc. Nephrol.* **8**:1942–1945.

12. Kelley, M.J., Jawien, W., Ortel, T.L., and Korczak, J.F. 2000. Mutation of MYH9, encoding non-muscle myosin heavy chain A, in May-Hegglin anomaly. *Nat. Genet.* **26**:106–108.

13. Seri, M., et al. 2000. Mutations in MYH9 result in the May-Hegglin anomaly, and Fechtner and Sebastian syndromes. The May-Hegglin/Fechtner Syndrome Consortium. *Nat. Genet.* **26**:103–105.

14. Heath, K.E., et al. 2001. Nonmuscle myosin heavy chain IIA mutations define a spectrum of autosomal dominant macrothrombocytopenias: May-Hegglin anomaly and Fechtner, Sebastian, Epstein, and Alport-like syndromes. *Am. J. Hum. Genet.* **69**:1033–1045.

15. Ghiggeri, G.M., et al. 2003. Genetics, clinical and pathological features of glomerulonephritis associated with mutations of nonmuscle myosin IIA (Fechtner syndrome). *Am. J. Kidney Dis.* **41**:95–104.

16. Arrondel, C., et al. 2002. Expression of the nonmuscle myosin heavy chain IIA in the human kidney and screening for MYH9 mutations in Epstein and Fechtner syndromes. *J. Am. Soc. Nephrol.* **13**:65–74.

17. Deller, T., et al. 2003. Synaptopodin-deficient mice lack a spine apparatus and show deficits in synaptic plasticity. *Proc. Natl. Acad. Sci. U. S. A.* **100**:10494–10499.

18. Putaala, H., Soininen, R., Kilpelainen, P., Wartiovaara, J., and Tryggvason, K. 2001. The murine nephrin gene is specifically expressed in kidney, brain and pancreas: inactivation of the gene leads to massive proteinuria and neonatal death. *Hum. Mol. Genet.* **10**:1–8.

19. Roselli, S., et al. 2004. Early glomerular filtration defect and severe renal disease in podocin-deficient mice. *Mol. Cell. Biol.* **24**:550–560.

20. Henderson, J.M., Al-Waheeb, S., Weins, A., Dandapani, S.V., and Pollak, M.R. 2008. Mice with altered alpha-actinin-4 expression have distinct morphologic patterns of glomerular disease. *Kidney Int.* **73**:741–750.

21. Huber, T.B., et al. 2006. Bigenic mouse models of focal segmental glomerulosclerosis involving pairwise interaction of CD2AP, Fyn, and synaptopodin. *J. Clin. Invest.* **116**:1337–1345.

22. Koop, K., et al. 2003. Expression of podocyte-associated molecules in acquired human kidney diseases. *J. Am. Soc. Nephrol.* **14**:2063–2071.

23. Zhang, S.Y., et al. 2004. In vivo expression of podocyte slit diaphragm-associated proteins in nephrotic patients with NPHS2 mutation. *Kidney Int.* **66**:945–954.

24. Brem, R.B., Yvert, G., Clinton, R., and Kruglyak, L. 2002. Genetic dissection of transcriptional regulation in budding yeast. *Science.* **296**:752–755.

25. Schadt, E.E., et al. 2003. Genetics of gene expression surveyed in maize, mouse and man. *Nature.* **422**:297–302.

26. Rockman, M.V., and Kruglyak, L. 2006. Genetics of global gene expression. *Nat. Rev. Genet.* **7**:862–872.

27. Hubner, N., et al. 2005. Integrated transcriptional profiling and linkage analysis for identification of genes underlying disease. *Nat. Genet.* **37**:243–253.

28. Wang, S., et al. 2006. Genetic and genomic analysis of a fat mass trait with complex inheritance reveals marked sex specificity. *PLoS Genet.* **2**:e15.

29. Schadt, E.E., et al. 2005. An integrative genomics approach to infer causal associations between gene expression and disease. *Nat. Genet.* **37**:710–717.

30. Chen, Y., et al. 2008. Variations in DNA elucidate molecular networks that cause disease. *Nature.* **452**:429–435.

31. Wyatt, C.M., and Klotman, P.E. 2007. HIV-1 and HIV-associated nephropathy 25 years later. *Clin. J. Am. Soc. Nephrol.* **2**(Suppl. 1):S20–S24.

32. D'Agati, V., and Appel, G.B. 1997. HIV infection and the kidney. *J. Am. Soc. Nephrol.* **8**:138–152.

33. Winston, J.A., et al. 2001. Nephropathy and establishment of a renal reservoir of HIV type 1 during primary infection. *N. Engl. J. Med.* **344**:1979–1984.

34. Wyatt, C.M., and Klotman, P.E. 2007. HIV-associated nephropathy in the era of antiretroviral therapy. *Am. J. Med.* **120**:488–492.

35. Bruggeman, L.A., et al. 2000. Renal epithelium is a previously unrecognized site of HIV-1 infection. *J. Am. Soc. Nephrol.* **11**:2079–2087.

36. Sunamoto, M., Husain, M., He, J.C., Schwartz, E.J., and Klotman, P.E. 2003. Critical role for Nef in HIV-1-induced podocyte dedifferentiation. *Kidney Int.* **64**:1695–1701.

37. Husain, M., et al. 2002. HIV-1 Nef induces proliferation and anchorage-independent growth in podocytes. *J. Am. Soc. Nephrol.* **13**:1806–1815.

38. Husain, M., D'Agati, V.D., He, J.C., Klotman, M.E., and Klotman, P.E. 2005. HIV-1 Nef induces dedifferentiation of podocytes in vivo: a characteristic feature of HIVAN. *AIDS.* **19**:1975–1980.

39. He, J.C., et al. 2004. Nef stimulates proliferation of glomerular podocytes through activation of Src-dependent Stat3 and MAPK1,2 pathways. *J. Clin. Invest.* **114**:643–651.

40. Lu, T.C., et al. 2008. HIV-1 Nef disrupts the podocyte actin cytoskeleton by interacting with diaphanous interacting protein. *J. Biol. Chem.* **283**:8173–8182.

41. Ross, M.J., Martinka, S., D'Agati, V.D., and Bruggeman, L.A. 2005. NF-kappaB regulates Fas-mediated apoptosis in HIV-associated nephropathy. *J. Am. Soc. Nephrol.* **16**:2403–2411.

42. Kiryluk, K., Martino, J., and Gharavi, A.G. 2007. Genetic susceptibility, HIV infection, and the kidney. *Clin. J. Am. Soc. Nephrol.* **2**(Suppl. 1):S25–S35.

43. Winston, J.A., Klotman, M.E., and Klotman, P.E. 1999. HIV-associated nephropathy is a late, not early, manifestation of HIV-1 infection. *Kidney Int.* **55**:1036–1040.

44. Kopp, J.B., et al. 1992. Progressive glomerulosclerosis and enhanced renal accumulation of basement membrane components in mice transgenic for human immunodeficiency virus type 1 genes. *Proc. Natl. Acad. Sci. U. S. A.* **89**:1577–1581.

45. Gharavi, A.G., et al. 2004. Mapping a locus for susceptibility to HIV-1-associated nephropathy to mouse chromosome 3. *Proc. Natl. Acad. Sci. U. S. A.* **101**:2488–2493.

46. Zhong, J., et al. 2005. Expression of HIV-1 genes in podocytes alone can lead to the full spectrum of HIV-1-associated nephropathy. *Kidney Int.* **68**:1048–1060.

47. Knott, S.A., and Haley, C.S. 2000. Multitrait least squares for quantitative trait loci detection. *Genetics.* **156**:899–911.

48. Frazer, K.A., et al. 2007. A sequence-based variation map of 8.27 million SNPs in inbred mouse strains. *Nature.* **448**:1050–1053.

49. Belknap, J.K. 2003. Chromosome substitution strains: some quantitative considerations for genome scans and fine mapping. *Mamm. Genome.* **14**:723–732.

50. Chan, K.T., et al. 2008. Accelerated development of collapsing glomerulopathy in mice congenic for the HIVAN1 locus. *Kidney Int.* **75**:366–372.

51. Mhatre, A.N., et al. 2007. Generation and characterization of mice with Myh9 deficiency. *Neuromolecular Med.* **9**:205–215.

52. Matsushita, T., et al. 2004. Targeted disruption of mouse ortholog of the human MYH9 responsible for macrothrombocytopenia with different organ involvement: hematological, nephrological, and otological studies of heterozygous KO mice. *Biochem. Biophys. Res. Commun.* **325**:1163–1171.

53. Ratelade, J., et al. 2008. Maternal environment interacts with modifier genes to influence progression of nephrotic syndrome. *J. Am. Soc. Nephrol.* **19**:1491–1499.

54. Takemoto, M., et al. 2006. Large-scale identification of genes implicated in kidney glomerulus development and function. *EMBO J.* **25**:1160–1174.

55. Rohr, C., et al. 2002. The LIM-homeodomain transcription factor Lmx1b plays a crucial role in podocytes. *J. Clin. Invest.* **109**:1073–1082.

56. Yvert, G., et al. 2003. Trans-acting regulatory variation in Saccharomyces cerevisiae and the role of transcription factors. *Nat. Genet.* **35**:57–64.

57. Park, C.C., et al. 2008. Fine mapping of regulatory loci for mammalian gene expression using radiation hybrids. *Nat. Genet.* **40**:421–429.

58. Ronald, J., Brem, R.B., Whittle, J., and Kruglyak, L. 2005. Local regulatory variation in Saccharomyces cerevisiae. *PLoS Genet.* **1**:e25.

59. GuhaThakurta, D., et al. 2006. Cis-regulatory variations: a study of SNPs around genes showing cis-linkage in segregating mouse populations. *BMC Genomics.* **7**:235.

60. Doss, S., Schadt, E.E., Drake, T.A., and Lusis, A.J. 2005. Cis-acting expression quantitative trait loci in mice. *Genome Res.* **15**:681–691.

61. Fay, J.C., and Wu, C.I. 2001. The neutral theory in the genomic era. *Curr. Opin. Genet. Dev.* **11**:642–646.

62. Pfaffl, M.W. 2001. A new mathematical model for relative quantification in real-time RT-PCR. *Nucleic Acids Res.* **29**:e45.

63. Manly, K.F., Cudmore, R.H., Jr., and Meer, J.M. 2001. Map Manager QTX, cross-platform software for genetic mapping. *Mamm. Genome.* **12**:930–932.

64. Lander, E., and Kruglyak, L. 1995. Genetic dissection of complex traits: guidelines for interpreting and reporting linkage results. *Nat. Genet.* **11**:241–247.

65. Broman, K.W., Wu, H., Sen, S., and Churchill, G.A. 2003. R/qtl: QTL mapping in experimental crosses. *Bioinformatics.* **19**:889–890.

66. Kumar, S., Tamura, K., and Nei, M. 2004. MEGA3: Integrated software for Molecular Evolutionary Genetics Analysis and sequence alignment. *Brief Bioinform.* **5**:150–163.

67. Doron-Faigenboim, A., Stern, A., Mayrose, I., Bacharach, E., and Pupko, T. 2005. Selecton: a server for detecting evolutionary forces at a single amino-acid site. *Bioinformatics.* **21**:2101–2103.